物理化学学报(Wuli Huaxue Xuebao)
第 26 卷第 10 期(2010 年 10 月)

目　　次

(下转封三)

(上接封二)

光化学与光谱

量子化学及计算化学

生物物理化学

材料物理化学

ACTA PHYSICO-CHIMICA SINICA
Vol. 26 No.10 (October, 2010)

CONTENTS

Review

THERMODYNAMICS, THERMOCHEMISTRY AND SOLUTION CHEMISTRY

CHEMICAL KINETICS AND MOLECULE DYNAMICS

Temperature Dependence of Reactions of $C_2(a^3\Pi_u)$ Radical with Several Unsaturated Hydrocarbons

HU Ren-Zhi ZHANG Qun
CHEN Yang

Acta Phys. -Chim. Sin., **2010, 26**(10): 2619–2624

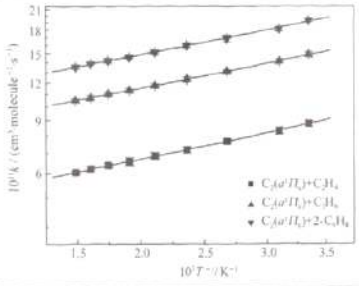

We studied a temperature dependence of the reactions of $C_2(a^3\Pi_u)$ with several unsaturated hydrocarbons (C_2H_4, C_2H_2, C_3H_6, and 2-C_4H_8).

ELECTROCHEMISTRY

Electrodeposition of Copper in a Citrate Bath and Its Application to a Micro-Electro-Mechanical System

WU Wei-Gang YANG Fang-Zu
LUO Ming-Hui TIAN Zhong-Qun
ZHOU Shao-Min

Acta Phys. -Chim. Sin., **2010, 26**(10): 2625–2632

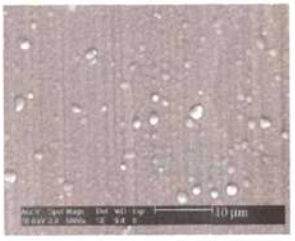

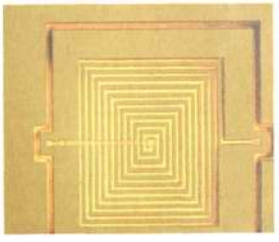

A copper coating was electrodeposited from a novel citrate bath and a planar inductor was successfully fabricated for MEMS in this bath.

Effect of Hydrazine on the Performance of $LiNi_{0.5}Mn_{1.5}O_4$ Cathode Materials

CHANG Zhao-Rong DAI Dong-Mei
LI Bao TANG Hong-Wei

Acta Phys. -Chim. Sin., **2010, 26**(10): 2633–2637

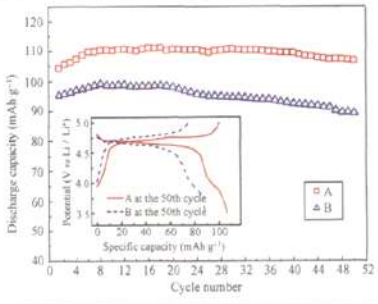

$LiNi_{0.5}Mn_{1.5}O_4$ was synthesized from a hydrazine pretreated precursor and it shows a much better electrochemical properties because of the formed pure spinel phase.

Characteristics of the Microbiologically Influenced Corrosion of 304 Stainless Steel in Reclaimed Water Enviroment

LI Jin XU Zhao-Yi
LI Jiu-Yi JIAO Di

Acta Phys. -Chim. Sin., **2010, 26**(10): 2638–2646

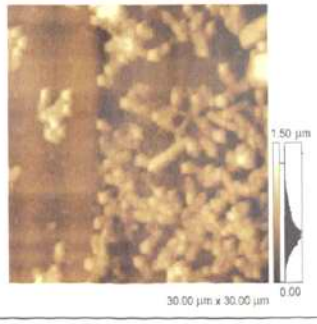

Because of the development of a biofilm on the surface of SS304, which resulted from the interactions between the SS304 surface and the biofilm, a corrosive pit appeared on the surface of SS304. This indicates that the SS304 surface suffered from microbiologically influenced corrosion.

Electropolymerization of Nickel Complexes with Schiff Bases: Effect of Sweep Rate on Anodic Polymerization

LI Jian-Ling GAO Fei
ZHANG Ya-Kun HE Li-Zhi
HAN Gui-Mei WANG Xin-Dong

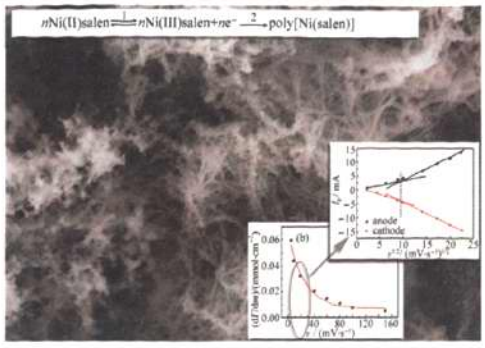

The active centers of poly[Ni(salen)] reach a maximum at a sweep rate of 20 mV·s^{-1} and it shows preferred diffusion kinetics.

Acta Phys. -Chim. Sin., **2010, 26**(10): 2647–2652

Preparation and Properties of Poly(vinyl alcohol)/Poly(vinyl pyrrolidone) Composites for Solid Alkaline Electrolyte Membranes

FU Jing LIN Rui
LÜ Hong WANG Xiao-Lei
MA Jian-Xin QIAO Jin-Li

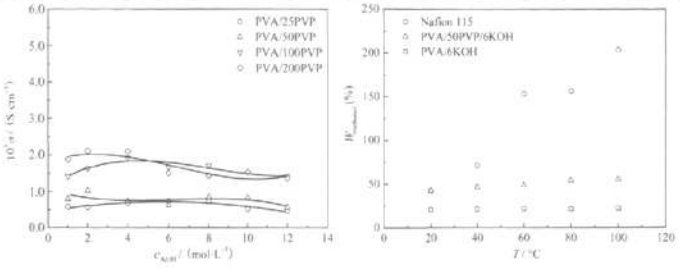

We obtained high ionic conductivity (2.01×10^{-3} S·cm^{-1}) for an alkaline PVA/ PVP membrane and it maintained good strength stability in a methanol solution at elevated temperatures.

Acta Phys. -Chim. Sin., **2010, 26**(10): 2653–2658

Electroosmotic Drag of Water in Hydrated Potassium Perfluorosulfonated Polymer Membrane in External Electric Fields

ZHU Su-Hua YAN Liu-Ming
JI Xiao-Bo SHAO Chang-Le
LU Wen-Cong

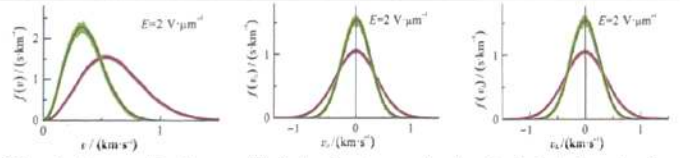

The electroosmotic drag coefficient of water molecules in hydrated potassium perfluorosulfonate membrane is analyzed from different coordination shells of the cation and evaluated from the Maxwall velocity distribution function and molecular dynamics simulations with an external electric field applied.

Acta Phys. -Chim. Sin., **2010, 26**(10): 2659–2665

COLLOID AND INTERFACE CHEMISTRY

Effect of Catalysts on the Morphologies of Carbon Materials Synthesized by an Emulsion Templating Method

GAN Li-Hua LIU Ming-Xian
CHEN Long-Wu HU Jun
LIU Hong-Lai

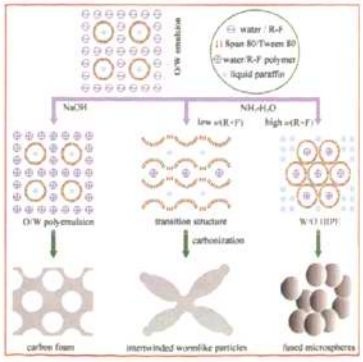

A phase inversion occurred in an O/W emulsion system and was caused by intermolecular H-bond interactions. Carbon foams and carbon materials consisting of fused microspheres or worm-like particles were prepared using NaOH and ammonia as catalysts, respectively.

Acta Phys. -Chim. Sin., **2010, 26**(10): 2666–2671

CATALYSIS AND SURFACE STRUCTURE

Study of Competitive Adsorption Behavior of Protein and Methylene Blue by Optical Waveguide Spectroscopy

DENG Lin QI Zhi-Mei

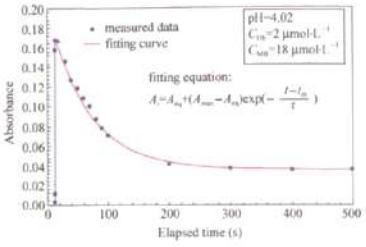

The competitive coadsorption of methylene blue (MB) and protein on hydrophilic glass was monitored *in situ* by time-resolved optical waveguide spectroscopy and the best fit of the measured time course of absorbance with the theoretical kinetic equation reveals that the number of adsorbed MB molecules decreases exponentially with time after reaching a maximum.

Acta Phys. -Chim. Sin., **2010, 26**(10): 2672–2678

NO_x Molecule Adsorption in [Ag]-MAPO-5 (M=Si, Ti) Molecular Sieves

LIU Jie-Xiang ZHANG Xiao-Guang
DUAN Zhong-Yu LIU Xiao-Li

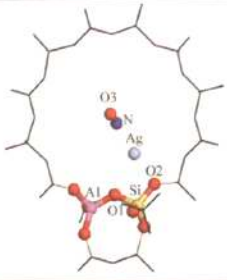

NO_x, SO_2, H_2O, and O_2 adsorption in [Ag]-MAPO-5 (M=Si, Ti) were investigated using the density functional theory (DFT). The natural bond orbital (NBO) analysis was performed to investigate the interaction mechanism of NO_x in the molecular sieves.

Acta Phys. -Chim. Sin., **2010, 26**(10): 2679–2685

Electric Field Assisted Hopping of *Tert*-Butylamine on Cu(111) Surface

XU Yu-Qun ZHANG Jun
YUAN Bing-Kai DENG Ke
YANG Rong QIU Xiao-Hui

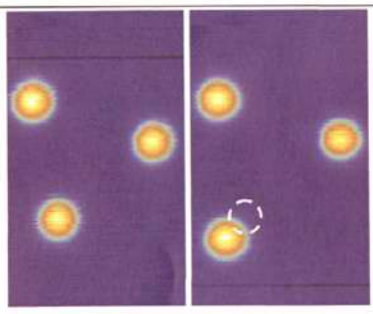

The hopping probabilities of *tert*-butylamine on Cu(111) surface present difference under the electric field of opposite polarity in an STM junction.

Acta Phys. -Chim. Sin., **2010, 26**(10): 2686–2690

Naphthalene Hydrogenation Activity over Pd, Pt and Pd-Pt Catalysts and Their Sulfur Tolerance

ZHANG Xiao-Fei SHAO Zheng-Feng
MAO Guo-Qiang HE De-Min
ZHANG Qiu-Min LIANG Chang-Hai

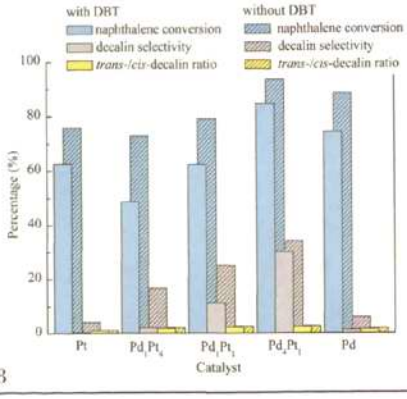

The Pd_4Pt_1 catalyst has the highest naphthalene conversion and best selectivity toward decalin among the studied Pd and Pt monometallic catalysts as well as the bimetallic Pd-Pt catalysts with molar ratios of 4:1, 1:1, and 1:4 in the presence and absence of dibenzothiophene (DBT).

Acta Phys. -Chim. Sin., **2010, 26**(10): 2691–2698

Activation Factors for the Carboxyl Group in the Hydrogenation of Carboxylic Esters

ZHENG Xiao-Juan ZHOU Ya-Fen
FU Hai-Yan CHEN Hua
LI Xian-Jun LI Rui-Xiang

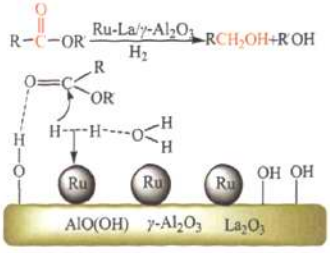

Water, $Co(NO_3)_2$, and an electron-withdrawing group all contributed to the activation of the carboxyl group in a carboxylic ester.

Acta Phys. -Chim. Sin., **2010, 26**(10): 2699–2704

Selective Oxidation of Ethylbenzene with Hydrogen Peroxide Catalyzed by 5,7-Dibromo-8-quinolinolato Manganese Complexes

LU Chun-Li FU Zai-Hui
LIU Ya-Chun LIU Feng-Lan
QIN Jin-Wei HE Xiang-Ling
YIN Du-Lin

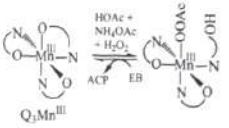

A 5,7-dibromo-8-quinolinolato manganese(III) complex (Q_3Mn^{III}) of changeable hexadentate mode, with the help of NH_4OAC and HOAc, was found to be an efficient catalyst for the selective oxidation of ethylbenzene (EB) to acetophenone (ACP) with aqueous hydrogen peroxide in environmentally benign acetone-water media.

Acta Phys. -Chim. Sin., **2010, 26**(10): 2705–2710

Asymmetric Hydrogenation of Acetophenone Catalyzed by $RuCl_2(TPP)_3$ Supported on Hydroxyapatite Modified with Chiral Amine

ZHANG Ding-Lin YANG Chao-Fen
SUN Ya-Ping FU Hai-Yan
LI Rui-Xiang CHEN Hua
LI Xian-Jun

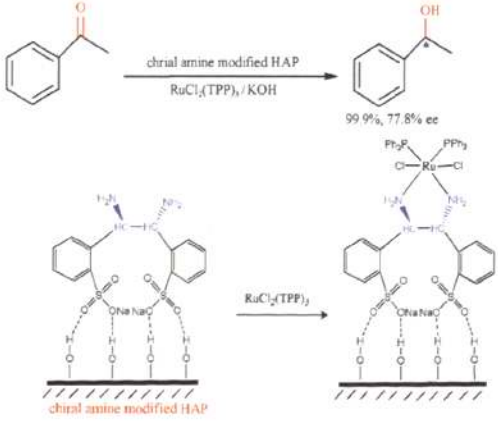

$RuCl_2(TPP)_3$ supported on (1*R*,2*R*)-DPENDS modified HAP was prepared and used to catalyze the asymmetric hydrogenation of acetophenone with high activity and enantioselectivity.

Acta Phys. -Chim. Sin., **2010, 26**(10): 2711–2718

1-Octene Hydroformylation Using Supported Amorphous Co-B Catalysts

LONG Jun-Ying MA Lan
HE De-Hua

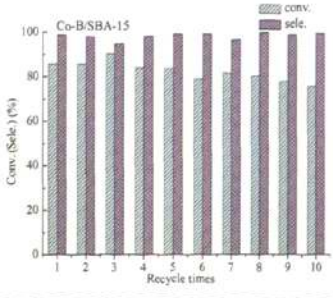

Supported Co-B catalysts showed high initial activity and selectivity in 1-octene hydroformylation and Co-B/SBA-15 showed relatively high stability during catalyst recycling.

Acta Phys. -Chim. Sin., **2010, 26**(10): 2719–2725

Preparation, Characterization and Photocatalytic Property of *p*-CoO/*n*-CdS Compound Semiconductor Photocatalyst

DU Huan WANG Sheng
LIU Lian-Lian LIU Zhong-Xiang
LI Zhen LU Nan
LIU Fu-Sheng

Acta Phys. -Chim. Sin., **2010, 26**(10): 2726–2732

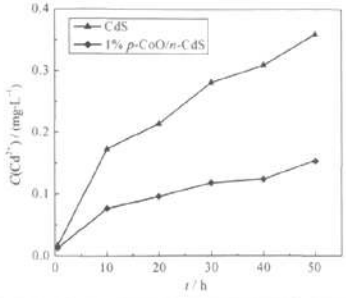

The photocatalyst CdS and CoO/CdS (*p*-CoO/*n*-CdS) compound semiconductor photocatalyst were prepared. The results of photocorrosion test showed that the photocorrosion rate of CdS was two or more times than that of *p*-CoO/*n*-CdS compound, which indicated that CoO coupled with CdS could effectively restrain the photocorrosion of CdS.

Photoinduced Charge Carrier Properties and Photocatalytic Activity of N-Doped TiO_2 Nanocatalysts

ZHANG Xiao-Ru LIN Yan-Hong
ZHANG Jian-Fu HE Dong-Qing
WANG De-Jun

Acta Phys. -Chim. Sin., **2010, 26**(10): 2733–2738

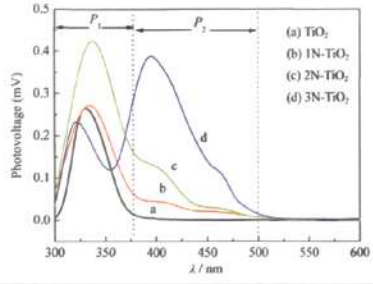

N-TiO_2 photocatalysts with an appropriate amount of N doping showed a higher separation efficiency for photoinduced charge carriers than TiO_2 photocatalysts.

Decomposition of N_2O on ACo_2O_4/HZSM-5 Catalysts

WANG Hong WANG Jun-Li
LI Cui-Qing SONG Yong-Ji
CHI Yao-Ling WANG Tao

Acta Phys. -Chim. Sin., **2010, 26**(10): 2739–2744

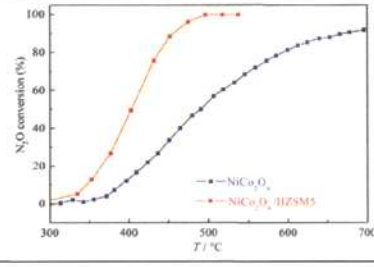

ACo_2O_4 (A=Mg, Ni, Zn) and ACo_2O_4/HZSM-5(A=Mg, Fe, Ni, Cu, Zn, Zr, La) catalysts were synthesized and the performance of the catalysts was characterized. Compared with ACo_2O_4, the ACo_2O_4/HZSM-5 catalyst had better catalytic activity.

PHOTOCHEMISTRY AND SPECTROSCOPY

Enhancing the Photovoltaic Performance of Dye Sensitized Solar Cells with the TiO_2 Sol Infiltrated Nanocrystalline Electrode

QIAN Di-Feng ZHANG Qing-Hong
WAN Jun LI Yao-Gang
WANG Hong-Zhi

Acta Phys. -Chim. Sin., **2010, 26**(10): 2745–2751

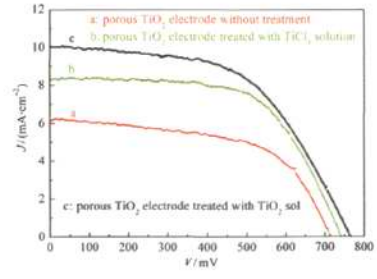

The overall energy conversion efficiency of the DSSCs was significantly enhanced by 64% after the low-concentration TiO_2 sol infiltrated to the porous TiO_2 photoanode.

Efficient Polymer White-Light-Emitting Devices Based on Two Complementary Phosphorescent Colors

LI Yan-Hu FANG Yuan
ZOU Jian-Hua WANG Biao
WU Hong-Bin PENG Jun-Biao

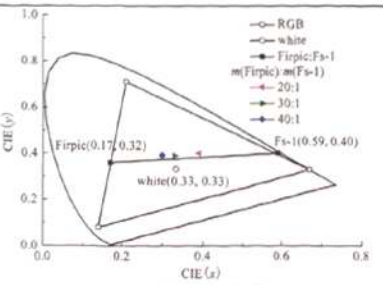

Efficient white polymer light-emitting diodes (WPLEDs) were fabricated by spin coating method using two complementary colors.

Acta Phys. -Chim. Sin., **2010, 26**(10): 2752–2756

Effects of NaCl on the Separation of Single-Walled Carbon Nanotubes by Agarose Gel Electrophoresis

WEN Xiao-Nan ZHANG Jing
GU Wen-Xiu JIN He-Hua
LI Hong-Bo LI Qing-Wen

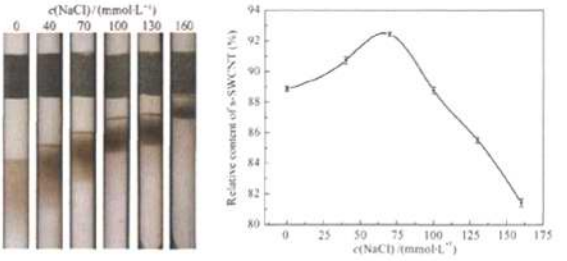

The effect of NaCl on the separation of m-SWCNT and s-SWCNT by agarose gel electrophoresis was investigated.

Acta Phys. -Chim. Sin., **2010, 26**(10): 2757–2762

QUANTUM CHEMISTRY AND COMPUTATION CHEMISTRY

Structure, Spectroscopy and Reactivity Properties of Helically Chiral Metal(II)-Bisdipyrrin Complexes

ZHONG Ai-Guo HUANG Ling
LI Bai-Lin JIANG Hua-Jiang
LIU Shu-Bin

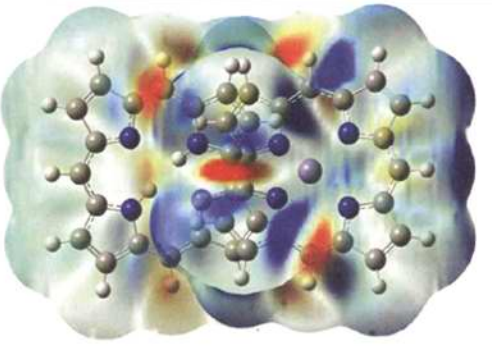

Knotted helical porphyrins metalated by a variety of divalent metal cations are investigated by conventional, time-dependent, and density functional theory approaches rendering a number of quantitative structure–reactivity linear relationships and other insights from structure and reactivity viewpoints.

Acta Phys. -Chim. Sin., **2010, 26**(10): 2763–2771

Characteristics of One Electron Redox Behavior of Hydrophobic Amino Acids in Gas Phase

LI Wei-Wei HOU Ruo-Bing
SUN Yan-Li

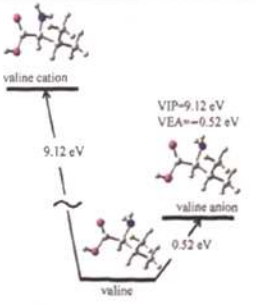

The lower redox activities of hydrophobic amino acids in gas phase are attributable to their high ionization potentials and negative electron affinities.

Acta Phys. -Chim. Sin., **2010, 26**(10): 2772–2778

Theoretical Investigation of the Key Reaction for the Chemiluminescence of Cypridina Luciferin Analogues

SUN Ying REN Ai-Min
MIN Chun-Gang ZOU Lu-Yi
REN Xue-Feng

We verify by theoretical calculations that MIPb (with 3-indolyl as the substituent) has a lower EEP and energy gap and a larger natural charge population change than other luciferin derivatives, and this is similar to cypridina luciferin in diglyme.

Acta Phys. -Chim. Sin., **2010, 26**(10): 2779–2786

Photodissociation Mechanism of Cyanogen Azide

CI Cheng-Gang DUAN Xue-Mei
LIU Jing-Yao SUN Chia-Chung

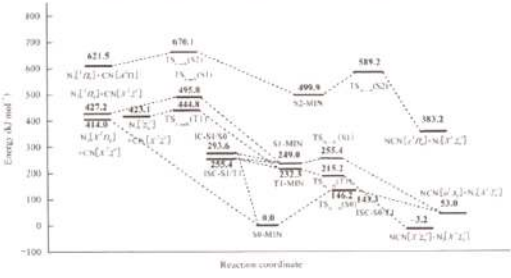

The photodissociation mechanism of N_3CN in the S0, T1, S1, and S2 states were investigated at the MRCI+Q//CAS(10, 9)/6-311+G(2*df*) level of theory.

Acta Phys. -Chim. Sin., **2010, 26**(10): 2787–2792

Atomic Partial Charges for Periodic Systems from First-Principles Calculations

LI Ya-Na LÜ Yang
ZHOU Li-Chuan CHEN Li
LI Shen-Min

We proposed a method to obtain atomic partial charges rapidly for periodic systems and we carried out least squares fitting of the electrostatic potential (ESP) from first-principles calculations and used this in the Ewald summation.

Acta Phys. -Chim. Sin., **2010, 26**(10): 2793–2800

Half-Metallic Properties of Mn-AlN and Cr-AlN Based on First-Principles

FAN Yu-Qin HE A-Ling

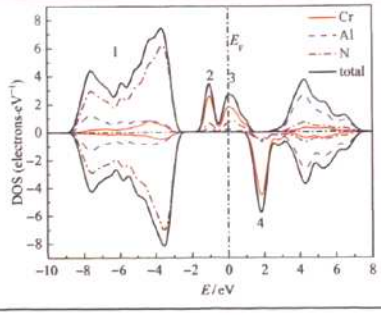

As the Mn/Cr doping concentration increases, the interaction between Mn and Mn or Cr and Cr atoms increases and the hybridization of the Mn/Cr 3*d* and N 2*p* states weakens, so the half-metallic gap is decreased.

Acta Phys. -Chim. Sin., **2010, 26**(10): 2801–2806

Effect of the Hydrodynamic Radius of Colloid Microspheres on the Estimation of the Coagulation Rate Constant

DU Xuan XU Sheng-Hua
SUN Zhi-Wei AA Yan

Acta Phys. -Chim. Sin., **2010, 26**(10): 2807–2812

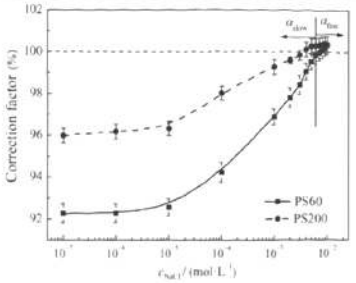

Coagulation rate constants calculated by using the hydrodynamic radius instead of the geometric radius can be lower than its theoretical value by up to 8% at low ionic strength and this difference decreases with the increase of ionic strength.

BIOPHYSICAL CHEMISTRY

Effects of Molecular Volume and Fractional Polar Surface Area of Osmolytes on the Thermal Stability of Chymotrypsin Inhibitor 2

LIU Fu-Feng JI Luo
DONG Xiao-Yan

Acta Phys. -Chim. Sin., **2010, 26**(10): 2813–2820

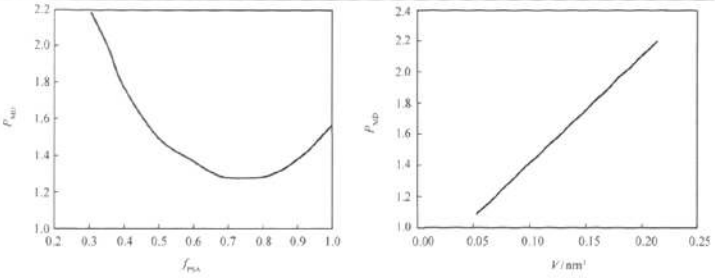

The molecular basis for the stabilizing effect of osmolytes was studied by molecular dynamics simulations. We found that the fractional polar surface area and the molecular volume determine their protective ability.

Effect of Surface Chemical Properties of a Silicon Chip on Antibody Immobilization

ZHOU Wen-Wen LIAN Jie
HU Ke-Jia GAO Yun-Hua
XU Bai

Acta Phys. -Chim. Sin., **2010, 26**(10): 2821–2827

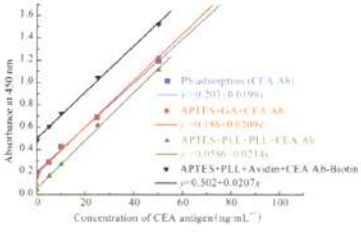

We found that the most efficient immobilization strategy was the use of glutaraldehyde as a coupling reagent to link a CEA antibody and an amino abundant surface that had been modified by a poly-L-lysine spacer-arm.

Specificity of Cation–π Interactions in Typical Protein Folds

QIAO Hui LI Xiao-Qin
XU Hai-Song KONG Ling-Qiang
PENG Yu

Fold type	$\overline{N_\pi(j)}$	$\overline{N(j)}$	$\overline{N_\pi(j)}$ / $\overline{N(j)}$	R
singly wound	4.91	326.03	1.51%	0.68
doubly wound	1.19	206.76	0.58%	0.05

In proteins, cation $-\pi$ interactions are formed between positively charged amino acids (Lys, Arg) and aromatic amino acids (Phe, Tyr, Trp). Cation–π interactions have existential specificity in typical protein folds.

Acta Phys. -Chim. Sin., **2010, 26**(10): 2828–2832

Homology Modeling and Structure Validation of the Adenosine A_1 Receptor

KE Yan-Rong JIN Hong-Wei
LIU Zhen-Ming ZHANG Liang-Ren

Acta Phys. -Chim. Sin., **2010, 26**(10): 2833–2839

We established the adenosine A_1 receptor model based on the adenosine A_{2A} receptor crystal structure and validated the models using DOCK, VINA, and GOLD softwares for virtual screening.

Structure and Formation Mechanism of Sn-Doped ZnO Nanoneedles

WANG Jie ZHUANG Hui-Zhao
XUE Cheng-Shan LI Jun-Lin
XU Peng

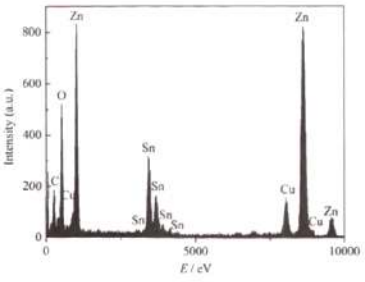

Sn-doped ZnO nanoneedles were synthesized in two steps: sputtering and thermal oxidation. These nanoneedles showed good luminescence characteristics.

Acta Phys. -Chim. Sin., **2010, 26**(10): 2840–2844

Synthesis and Properties of Amphiphilic Photosensitive Telechelic Polymer C-PNIPAAm

SHU Qiao-Zhen CHEN Xin
CHEN Kai-Hua JIANG Jin-Qiang
NI Zhong-Bin ZHANG Hong-Wu
LIU Xiao-Ya CHEN Ming-Qing

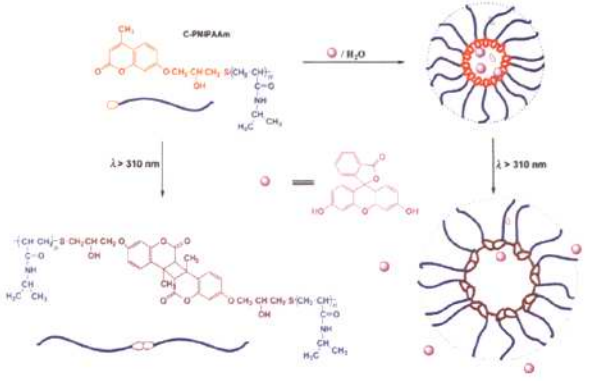

A coumarin-containing telechelic C-PNIPAAm polymer was used to form micelles in water with fluorescein as a hydrophobic agent. When irradiated by UV light (λ>310 nm), the hydrophobic coumarin unit at the end of the polymer chain was photodimerized, which resulted in a change in the micelle structure and the effective release of hydrophobic fluorescein into water.

Acta Phys. -Chim. Sin., **2010, 26**(10): 2845–2850

Effect of Natural Impurities on the Electronic Structures and Semiconducting Properties of Sphalerite

CHEN Ye CHEN Jian-Hua
GUO Jin

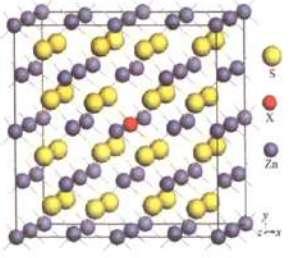

A systematic study of the electronic structures and semiconducting properties of sphalerite containing fourteen kinds of natural impurities was performed.

Acta Phys. -Chim. Sin., **2010, 26**(10): 2851–2856